Available online at www.sciencedirect.com
ScienceDirect
Dyes and Pigments 75 (2007) 633–640
DYES and PIGMENTS
www.elsevier.com/locate/dyepig

# The synthesis and spectral properties determination of 1,3-substituted phenyl-5-phenylformazans

Habibe Tezcan*, Elif Uzluk

*Department of Chemistry, Gazi University, Faculty of Gazi Education, Teknikokullar, 06500 Ankara, Turkey*

Received 26 June 2006; received in revised form 6 July 2006; accepted 6 July 2006
Available online 6 September 2006

**Abstract**

In this study, novel 1,3-substituted phenyl-5-phenylformazans were synthesized with $-NO_2$, $-Cl$, $-Br$, $-CH_3$, $-OCH_3$ groups in the *o*-, *m*-, and *p*-position of the 1-phenyl ring and $-NO_2$, $-OCH_3$ groups in the *m*- and *p*-position of the 3-phenyl ring. Their structures were elucidated by elemental analysis and GC–mass and their spectral behaviors were investigated with $^1H$ NMR, $^{13}C$ NMR, IR, UV–vis spectra. The absorption characteristics of the compounds were examined by UV–vis spectra. There was a shift in $\lambda_{max}$ whose amount was dependent upon the type and position of the substituent on the ring. A linear correlation was obtained between this substituent effect and Hammett substituent coefficients.


*Keywords:* Formazan dyes; Spectroscopy; Substituent effect

## 1. Introduction

Formazans are coloured compounds due to the π–π* transitions; their color ranges from cherry red to red-violet. Since Von Pechman synthesized the first formazans [1], there have been numerous formazans synthesized and their structural features, tautomeric and photochromic isomers have been investigated [2–5]. In recent years crown formazans have been much studied due to their interesting chelate structures [6,7] which can be utilized as ion selective electrodes due to holes in their structures [8].

Several studies on the synthesis of complexes [9,10] have appeared. The redox behavior of such complexes has also been evaluated. Formazans form the corresponding tetrazolium salt when oxidized [11], tetrazolium salts are reduced back to formazans. The tetrazolium–formazan system is classified as a marker of vitality [12] and has been used to screen anti-cancer drugs and to determine the activity of tumor cells [13,14] as well as to determine sperm viability [15]. Although formazans have other important medical applications, they are toxic in nature which prevented its routine in health sector. The aim of this study was to synthesize less toxic compounds for medical use.

The spectral behavior of some formazans has also been investigated [16]. In our previous work we synthesized various formazans and bis-formazans with electron donating and withdrawing groups attached to the 1,3,5-phenyl ring and investigated the effects of substituents on $\lambda_{max}$ [17–20]; nitro derivatives [21] as well as bis-formazans have been studied [22].

In this work, novel formazans with various substituents attached at the 1- and 3-phenyl rings have been synthesized (Fig. 1), their structures were elucidated and their spectral behavior was investigated using elemental analysis, mass, $^1H$ NMR, $^{13}C$ NMR, IR, UV–vis spectra. The effect of substituents was also determined, $\lambda_{max}$ shift values, by the use of UV–vis spectra.

## 2. Results and discussion

### 2.1. Synthesis of formazans

There are three distinctive routes proposed for the synthesis of formazans in the literature. The first one is the condensation

* Corresponding author. Tel.: +90 312 2126470x3909; fax: +90 312 2228483.
*E-mail address:* habibe@gazi.edu.tr (H. Tezcan).

0143-7208/$ - see front matter © 2006 Elsevier Ltd. All rights reserved.
doi:10.1016/j.dyepig.2006.07.011

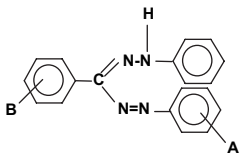


| Compound | A | B | Abbreviation | Compound | A | B | Abbreviation |
|---|---|---|---|---|---|---|---|
| 1 | H | H | TPF | 9 | m-Br | m-$NO_2$ | m-BNF |
| 2 | *o*-$NO_2$ | *m*-$NO_2$ | o-NNF | 10 | p-Br | m-$NO_2$ | p-BNF |
| 3 | *o*-$NO_2$ | *m*-$NO_2$ | m-NNF | 11 | o-$CH_3$ | p-$OCH_3$ | o-MMOF |
| 4 | *o*-$NO_2$ | *m*-$NO_2$ | p-NNF | 12 | m-$CH_3$ | p-$OCH_3$ | m-MMOF |
| 5 | *o*-Cl | m-$NO_2$ | o-CNF | 13 | p-$CH_3$ | p-$OCH_3$ | p-MMOF |
| 6 | *m*-Cl | m-$NO_2$ | m-CNF | 14 | o-$OCH_3$ | p-$OCH_3$ | o-MOF |
| 7 | *p*-Cl | m-$NO_2$ | p-CNF | 15 | m-$OCH_3$ | p-$OCH_3$ | m-MOF |
| 8 | *o*-Br | m-$NO_2$ | o-BNF | 16 | p-$OCH_3$ | p-$OCH_3$ | p-MOF |

Fig. 1. The structure of the formazan derivatives.

of aromatic and aliphatic aldehydes with phenylhydrazine and the coupling reaction of the resulting hydrazones with diazonium salts. This is a low yield route and the purification of the products is cumbersome and requires patience. The second way involves the coupling of active methylene compounds with 2 mol of diazonium cations. This is highly practical and easy but only gives symmetrical formazans [5,16]. The third method employs phase transfer, but requires special and expensive solvents such as crown ethers and tetrabutyl ammonium bromide [5].

In this work, formazans were synthesized using the first method, namely the coupling of hydrazones with diazonium cations in basic media at −5−0 °C (Scheme 1). The necessary hydrazones were obtained by the condensation reaction of benzaldehyde (or substituted benzaldehydes) and phenylhydrazine at pH 5−6.

The reason for the preference of this method, despite the inherent problem, is that the starting material is readily available and it has the advantage of synthesizing both symmetrical and asymmetrical formazans [16,17]. We tried to increase the yield in order to provide a cheap way to synthesize formazans.

The *basic buffer solutions* employed were 0.1 M $HClO_4$ + 0.05 M borax solution (pH 7.60 − 9.00) and 0.1 M NaOH + 0.05 M borax solution (pH 9.30 − 10.80). However, the best yield was obtained with the NaOH + $CH_3COONa$ buffer solution (pH 10 − 12). The formation mechanism for the substituted formazans is given in Scheme 1 and the experimental data are tabulated in Table 1. The structures of the formazans were elucidated by elemental analysis, mass spectroscopy, IR, $^1H$ NMR, $^{13}C$ NMR and UV−vis spectra. All the data were as expected.

As Table 1 shows, the yield of TPF is higher than that reported in the literature [18,19]. The reason that the lowest yield was obtained at the *o*-position on the 1-phenyl ring can be attributed to the substituent being close to the reaction site, which sterically hinders the coupling reaction. The relative increase in yield at both the *m*- and *p*-position (on the 1-phenyl ring) verifies this diagnosis. However, the substitution of $-CH_3$, and $-OCH_3$ at the *m*-position of the 1-phenyl ring reduced the yield. These compounds gave a sticky gummy product. Also the formazans with the *m*-substituted $-CH_3$ and $-OCH_3$ groups were difficult to synthesize; the mixing process needed to be terminated at the drop wise addition of diazonium to hydrazone product. Each product was crystallized from methanol.

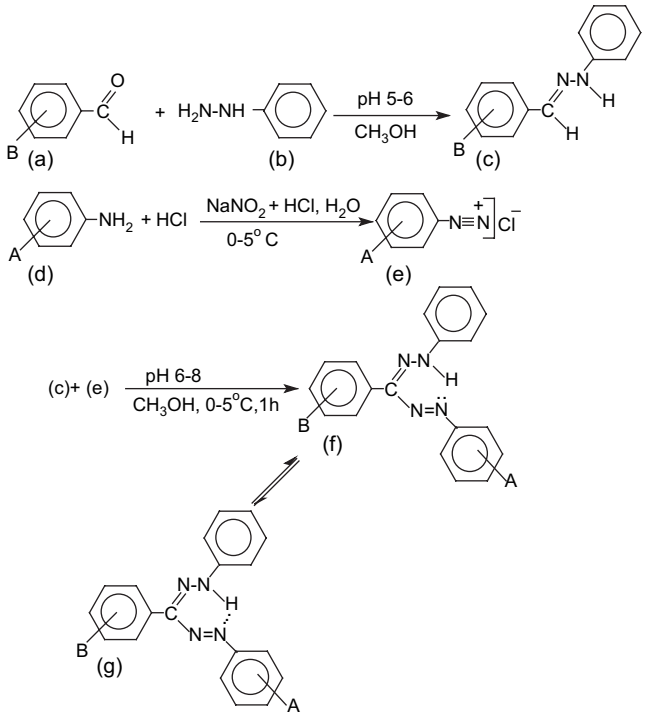


Scheme 1. The formation mechanism of formazans.

## 2.2. Spectral properties

When one examines the $^1H$ NMR data listed in Table 1, it is evident that the aromatic-H and NH peaks for TPF (**1**) were observed at $\delta = 8.37-7.27$ ppm and $\delta = 1.18$ ppm. Normally one would expect a single aromatic-H peak at $\delta = 7.27$ ppm. The weak electron withdrawal effect of the other phenyl rings and the double bond resonance in the structure of the formazan caused the aromatic-H peak to shift towards lower fields. This is an expected outcome [24].

In formazans **2−10** the position of 3-phenyl ring is substituted with *m*-$NO_2$ while $-NO_2$, −Cl and −Br are each substituted with the *o*-, *m*- and *p*-position of the 1-phenyl ring; the aromatic-H signals are shifted towards lower fields. This is in good accordance with the electron withdrawing properties of these substitutes. The fact that the order of shift was $o > p > m$ accords well with the inductive and resonance effects expected in these positions. This verifies the structure of the compounds.

In formazans **10−16** where the 1- and 3-phenyl rings are substituted with the electron donating *o*-$CH_3$ and $-OCH_3$ groups, the aromatic-H signals shifted to higher fields. This can also be explained with the inductive and resonance effects of the groups substituted at *o*-, *m*- and *p*-position. The

Table 1
Experimental and $^1$H NMR data of the formazans investigated

| Compounds | Color | Mp (°C) (lit.) | Yield % (lit) | $^1$H NMR data[a] | | | |
|---|---|---|---|---|---|---|---|
| | | | | Aromatic-H, $\delta$ (ppm) | Azo H, $\delta$ (ppm) | Methyl-H, $\delta$ (ppm) | Methoxy-H, $\delta$ (ppm) |
| **1** | Cherry red | 172–173 (172–174) | 78 (71) | 8.37–7.27 (15H) m | 1.18 (1H) s | | |
| **2** | Red-brown | 202–203 | 65 | 8.90–7.21 (13H) | 1.25 (1H) s | | |
| **3** | Red-brown | 190–191.5 | 67 | 8.55–7.42 (13H) | 1.58 (1H) | | |
| **4** | Dark purplish red | 195.5–197 | 71 | 8.78–7.09 (13H) | 2.51 (1H) | | |
| **5** | Red | 175.5–176.5 | 65 | 9.03–7.14 (13H) | 1.6 (1H) | | |
| **6** | Dark pink-red | 181.5–183 | 74 | 8.92–7.21 (13H) | 1.65 (1H) | | |
| **7** | Dark pink-red | 177.5–179 | 72 | 8.96–7.27 (13H) | 1.59 (1H) | | |
| **8** | Dark orange-red | 135–136.5 | 68 | 9.01–7.08 (13H) | 1.60 (1H) | | |
| **9** | Dark red | 145–146 | 73 | 8.85–6.93 (13H) | 2.68 (1H) | | |
| **10** | Orange-red | 176.5–177.5 | 70 | 8.94–7.28 (13H) | 2.24 (1H) | | |
| **11** | Red-pink | 187–188 | 69 | 8.21–6.97 (13H) | 1.60 (1H) | 2.56 (3H) | 3.90 (3H) |
| **12** | Purple-red | 210–211 | 40 | 8.42–6.40 (13H) | 1.30 (1H) | 2.44 (3H) | 3.88 (3H) |
| **13** | Dark purple | 242–243 | 74 | 8.16–6.78 (13H) | 1.58 (1H) | 2.45 (3H) | 3.90 (3H) |
| **14** | Dark purple | 196–197 | 71 | 8.26–6.83 (13H) | 1.31 (1H) | | 4.01–3.96 (6H) |
| **15** | Red-dark purple | 205–206.5 | 42 | 8.38–6.58 (13H) | 1.30 (1H) | | 3.91–3.84 (6H) |
| **16** | Dark purple | 187–188 | 72 | 8.12–6.87 (13H) | 1.31 (1H) | | 3.90–3.82 (6H) |

[a] The $^1$H NMR spectra were recorded at 400 MHz (in $CDCl_3$).

hydrogens of the $-CH_3$ and $-OCH_3$ groups appeared at their expected positions.

When one examines the $^{13}$C NMR data listed in Table 2 there is a 9C signal in contrast to the expected 13C signal for TPF. This shows that TPF is in its tautomeric form. The formation of a hydrogen bond between the electron pair on $-N=\ddot{N}-\phi$ and the hydrogen of NH turns the molecule into chelate structure and causes the tautomerism (Scheme 2) [2,18].

Table 2
$^{13}$C NMR data of the formazans investigated (100 MHz, in $CDCl_3$ and DMSO)

| Compounds | $\delta$ (ppm) | |
|---|---|---|
| | Imino-C (C=N) | Other carbons |
| **1** | 148.80 | 141.98, 138.28, 130.24, 129.21, 128.44, 128.29, 126.62, 119.54 (total 9C) |
| **2** | 149.98 | 148.53, 147.02, 145.91, 142.50, 141.62, 138.20, 135.77, 132.56, 130.64, 126.32, 124.83, 123.07, 121.33, 120.54, 118.85, 112.04 (total 17C) |
| **3** | 149.67 | 149.34, 148.57, 146.25, 139.78, 138.41, 132.43, 131.29, 130.54, 130.28, 129.61, 123.48, 122.73, 121.92, 121.64, 120.91, 112.63 (total 17C) |
| **4** | 149.76 | 148.09, 147.50, 145.71, 142.50, 137.38, 136.90, 134.52, 130.71, 129.64, 128.04, 127.26, 125.95, 120.00 118.09 (total 15C) |
| **5** | 150.82 | 149.66, 142.57, 140.93, 140.02, 136.35, 132.17, 131.29, 130.38, 130.10, 128.97, 127.21, 124.92, 123.05, 121.95, 121.32, 116.67 (total 17C) |
| **6** | 149.62 | 149.34, 148.14, 140.03, 139.75, 136.37, 132.09, 131.36, 130.41, 130.09, 127.57, 124.40, 123.03, 121.24, 120.80, 118.45, 117.03 (total 17C) |
| **7** | 149.65 | 147.83, 147.13, 141.85, 139.94, 134.53, 132.02, 130.42, 130.07, 129.05, 124.62, 122.92, 121.18, 120.95, 119.62 (total 15C) |
| **8** | 150.41 | 149.64, 144.31, 141.95, 140.69, 140.04, 133.79, 132.15, 130.88, 130.34, 129.53, 127.99, 123.02, 121.68, 121.30, 117.17, 115.67 (total 17C) |
| **9** | 149.62 | 149.28, 148.27, 142.27, 139.88, 132.09, 131.63, 130.41, 130.37, 128.06, 124.24, 123.03, 121.43, 121.24, 120.78, 118.06, 117.46 (total 17C) |
| **10** | 149.61 | 148.19, 147.11, 139.87, 133.48, 131.98, 130.23, 129.37, 124.89, 122.91, 122.11, 121.13, 120.91, 119.90, 116.70 (total 15C) |
| **11** | 160.46 | 149.93, 146.37, 144.80, 139.46, 131.64, 131.27, 130.26, 129.73, 128.78, 127.40, 124.66, 120.05, 114.98, 114.53, 55.71, 23.42 (total 17C) |
| **12** | 160.80 | 147.36, 141.97, 138.42, 132.63, 131.05, 130.00, 127.63, 126.97, 123.02, 120.78, 119.47, 116.05, 114.47, 112.63, 56.00, 22.80 (total 17C) |
| **13** | 160.39 | 148.88, 146.96, 141.96, 140.33, 131.13, 130.84, 130.18, 128.04, 126.15, 124.00, 120.96, 114.48, 55.71, 21.56 (total 15C) |
| **14** | 160.36 | 151.81, 150.25, 142.87, 138.57, 135.40, 131.46, 130.66, 129.33, 127.92, 126.27, 122.35, 121.54, 114.94, 114.50, 111.59, 55.98 (total 17C) |
| **15** | 164.50 | 160.02, 147.51, 145.01, 140.07, 138.96, 137.02, 134.57, 132.50, 131.00, 126.54, 120.06, 119.10, 116.07, 114.12, 112.19, 55.90 (total 17C) |
| **16** | 162.84 | 160.37, 147.08, 145.17, 141.86, 138.82, 131.11, 130.18, 128.12, 127.34, 124.27, 116.09, 115.31, 114.45, 55.70 (total 15C) |

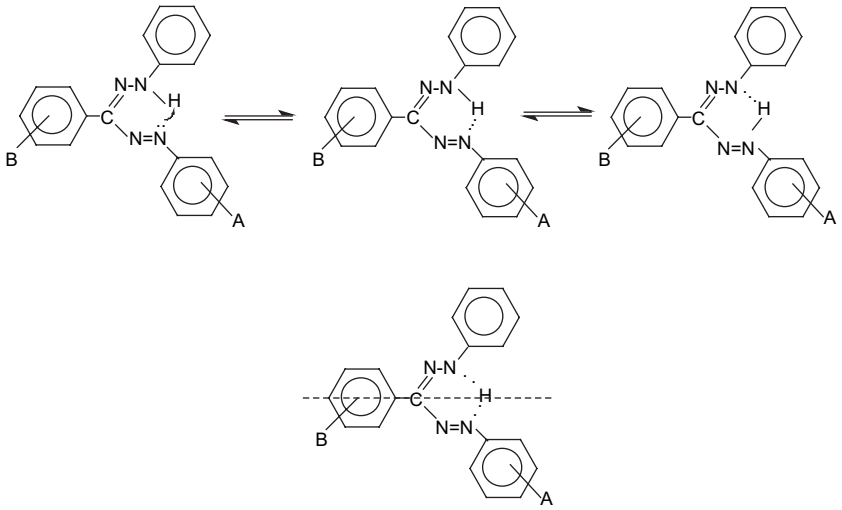


Scheme 2. Molecular chelation and symmetry.

From the $^{13}C$ NMR values of the substituted formazans **2**–**10** it is observed that the *p*-substituted compounds gave 15C signals and *o*- and *m*-substituted compounds gave 17C signal. In compounds **10**–**16** one would expect two more C due to the presence of $-CH_3$ and $-OCH_3$ substituents due to the fact that a symmetry plane is formed because *o*-$CH_3$ group is substituted at the *p*-position of 3-phenyl ring; there were 15C in compounds where the *p*-position of 1-phenyl ring is substituted (**13** and **16**) and 17C signal where the 1-penyl ring is *o*- or *m*-substituted (compounds **11**, **12**, **14**, and **15**) [24].

The *IR data* of formazans (**1**–**16**) given in Table 3 reveal the C=N stretching band at 1500–1530 $cm^{-1}$. However, when 1-phenyl ring is substituted with bulky groups such as $-NO_2$, −Cl, and −Br these groups push the 5-phenyl rings. Hence, in the case of formazans where the 5-phenyl ring is substituted with these groups (**1**–**10**) the C=N stretching band occurs at 1520–1530 $cm^{-1}$, indicating that the chelate and non-chelate structures are in equilibrium. The C=N stretching band appears at 1565–1551 $cm^{-1}$ in the case where there is no chelate structure present (excited state) and 1510–1500 $cm^{-1}$ in the case of chelation [3,23,25]. Therefore, formazans **11**–**16** must be extensively present in the chelate structure since the C=N stretching band appears at 1510–1500 $cm^{-1}$. Other IR data can be evaluated in a similar manner: aromatic C–H, C=C, and formazan specific CNNC stretching peaks and N–H, $-NO_2$, −Cl, −Br, $-CH_3$ and $-OCH_3$ vibration bands were observed in the expected regions [25].

### 2.3. Substituent effect on the UV–vis absorption $\lambda_{max}$ values

Table 4 lists all of the peaks observed in the UV–vis region of the formazan and substituted formazans **1**–**16**. Formazan peaks' $\lambda_{max1}$ values are generally observed at 410–500 nm and may be shifted to 550–600 nm depending upon the structure. These peaks are due to π–π* and n–π* electronic transitions in formazan skeleton. The $\lambda_{max2}$ peaks are sharp

Table 3
The IR spectral data of formazans **1**–**16** (KBr, $cm^{-1}$)

| Compound | Aromatic C–H | N–H | Aromatic C=C | C=N | $-NO_2$ | $-CH_3$ and $-OCH_3$ | N=N | CNNC structural vibration |
|---|---|---|---|---|---|---|---|---|
| **1** | 3069 | 3050–3000 | 1600 | 1500 | – | – | 1450 | 930–905 |
| **2** | 3500–3400 | 3060–3050 | 1600 | 1520–1540 | 1480 | – | 1350 | 890–680 |
| **3** | 3500–3410 | 3060–3050 | 1600 | 1530 | 1520 | – | 1350 | 800–650 |
| **4** | 3500–3400 | 3120–3080 | 1600 | 1520 | 1440 | – | 1340 | 820–640 |
| **5** | 3500–3410 | 3100–2900 | 1600 | 1530 | 1350 | – | 1250 | 820–650 |
| **6** | 3500–3400 | 3100–3080 | 1600 | 1530 | 1350 | – | 1250 | 820–680 |
| **7** | 3480–3400 | 3120–3080 | 1600 | 1520 | 1350 | – | 1250 | 890–680 |
| **8** | 3490–3410 | 3100–3070 | 1610 | 1520 | 1340 | – | 1250 | 810–650 |
| **9** | 3490–3410 | 2950–2850 | 1610 | 1520 | 1350 | – | 1220 | 800–650 |
| **10** | 3490–3410 | 2950–2850 | 1610 | 1520 | 1350 | – | 1220 | 800–650 |
| **11** | 3480–3400 | 2920–2800 | 1600 | 1500 | – | 1220 | 1030 | 800–620 |
| **12** | 3490 | 3020–3010 | 1620 | 1495 | – | 1200 | 1020 | 850–600 |
| **13** | 3440–3450 | 2950–2820 | 1600 | 1500 | – | 1250 | 1010 | 840–540 |
| **14** | 3490–3400 | 2900–2800 | 1600 | 1510 | – | 1250 | 1020 | 800–610 |
| **15** | 3490–3400 | 3030 | 1600 | 1505 | – | 1210 | 1030 | 810–580 |
| **16** | 3490 | 3050–3000 | 1600 | 1495 | – | 1250 | 1080 | 810–510 |

Table 4
UV–vis absorption maxima of formazans **1–16** ($CH_3COCH_3$, $10^{-5}$ mol $l^{-1}$)

| Compound | Abbreviation | $\lambda_{max1}$ (nm) (Abs) | $\lambda_{max2}$ (nm) (Abs) | Chemical shift $\Delta\lambda_{max}$ |
|---|---|---|---|---|
| **1** | TPF | 482.0 (0.630) | 380.0 (0.232) | – |
| **2** | *o*-$NO_2$, *m*-$NO_2$ | 484.0 (0.650) | 423.0 (0.275) | −2 |
| **3** | *m*-$NO_2$, *m*-$NO_2$ | 473.0 (0.402) | 406.0 (0.197) | 9 |
| **4** | *p*-$NO_2$, *m*-$NO_2$ | 478.0 (0.610) | 402.0 (0.338) | 4 |
| **5** | *o*-Cl, *m*-$NO_2$ | 482.0 (0.987) | 405.0 (0.264) | 0 |
| **6** | *m*-Cl, *m*-$NO_2$ | 479.0 (0.852) | 395.0 (0.179) | 3 |
| **7** | *p*-Cl, *m*-$NO_2$ | 486.0 (1.167) | 399.0 (0.212) | −4 |
| **8** | *o*-Br, *m*-$NO_2$ | 483.0 (0.318) | 423.0 (0.172) | −1 |
| **9** | *m*-Br, *m*-$NO_2$ | 480.0 (0.650) | 406.0 (0.263) | 2 |
| **10** | *p*-Br, *m*-$NO_2$ | 486.0 (0.630) | 405.0 (0.223) | −4 |
| **11** | *o*-$CH_3$, *p*-$OCH_3$ | 512.0 (0.625) | 406.0 (0.065) | −30 |
| **12** | *m*-$CH_3$, *p*-$OCH_3$ | 504.0 (0.046) | 446.0 (0.078) | −22 |
| **13** | *p*-$CH_3$, *p*-$OCH_3$ | 501.0 (0.379) | 399.0 (0.088) | −19 |
| **14** | *o*-$OCH_3$, *p*-$OCH_3$ | 531.0 (0.691) | 412.0 (0.080) | −49 |
| **15** | *m*-$OCH_3$, *p*-$OCH_3$ | 507.0 (0.015) | 414.0 (0.046) | −25 |
| **16** | *p*-$OCH_3$, *p*-$OCH_3$ | 499.0 (0.818) | 409.0 (0.253) | −17 |

Column 5: $\Delta\lambda_{max} = \lambda_{max1}(TPF) - \lambda_{max1}$ (substituted formazans).

and appear at 300–350 nm, corresponding to electronic transitions of –N=N– group in the molecule. The $\lambda_{max3}$ peaks observed at 270–300 nm originate from the n–$\pi^*$ transitions of –C=N– groups on the molecule. These are similar to those corresponding to –N=N– peaks in appearance.

Our discussion will focus on $\lambda_{max1}$ values, which are characteristic of the formazan structure. The chemical shift values ($\Delta\lambda$) were determined by taking the difference between the $\lambda_{max1}$ value of TPF and $\lambda_{max1}$ values of substituted formazans.

As seen in Table 4, *the* $\lambda_{max}$ value of TPF is 482 nm. However, these values were observed to be 484, 473 and 478 nm when the 1-phenyl ring is substituted with a $-NO_2$ group at the *o*-, *m*- and *p*-position, respectively, while the 3-phenyl ring is substituted with a $-NO_2$ group at the *m*-position (compounds **2–4**). The fact that $\lambda_{max1}$ of compound **2** shows a slight shift towards higher wavelength compared to TPF is not in good accordance with the electron withdrawing effect of the $-NO_2$ group. This can only be explained by the formation of a H-bond N–H hydrogen and oxygen of a $-NO_2$ group attached to the *o*-position of the 1-phenyl ring (Scheme 3). This diminishes the resonance effect of *o*-$NO_2$ group and decreases its electron withdrawing effect. This situation was described previously [19].

Both the *m*- and *p*-$NO_2$ substituted formazans (compounds **3** and **4**) do not display the strong electron withdrawing effect expected from $-NO_2$ group; indeed, it is acting as a weak electron withdrawing group. This situation verifies the assumption of the formation of H-bonds we made above. The shifts in absorption values ($\Delta\lambda_{max}$) of *m*- and *p*-$NO_2$ were merely 9 and 4 nm. This is attributed to the fact that there is no resonance effect and only a weak inductive effect with *m*-substitution while there was only very diminished inductive effect with *p*-substitution. These results are shown in Fig. 2a by comparing to TPF.

In both the –Cl and *o*-Br substituted compounds **5** and **8** the $\lambda_{max}$ value was shifted to 482 nm in the case of –Cl and 484 nm in the case of –Br due to the facts that their inductive electron withdrawing and resonance electron donating effects impose an opposing effect on each other. These effects cancel out each other for *o*-Cl substitution since electron withdrawing inductive effect and electron donating resonance effect of Cl are approximately the same. For the case of *o*-Br substitution the electron withdrawing inductive effect is smaller than Cl due to lower electronegativity of Br atom. Therefore, the resonance effect is slightly higher and Br acts as a weak electron donating group. These results are expected outcomes. Since there is no resonance effect at *m*-position they act as electron withdrawing group due to a weak inductive effect and shifted the $\lambda_{max}$ value slightly to lower wave lengths (479 nm for Cl and 480 nm for Br). It is natural that Cl shifted $\lambda_{max1}$ 1 nm less than Br and is due to the difference in their electronegativity values. At *p*-position both substituents shifted $\lambda_{max1}$

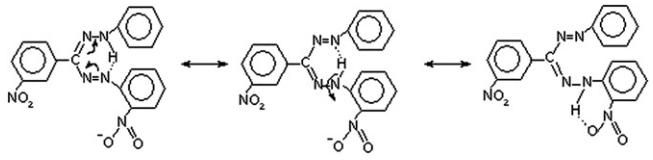


Scheme 3. The formation of hydrogen bond between the $-NO_2$ and N–H groups.

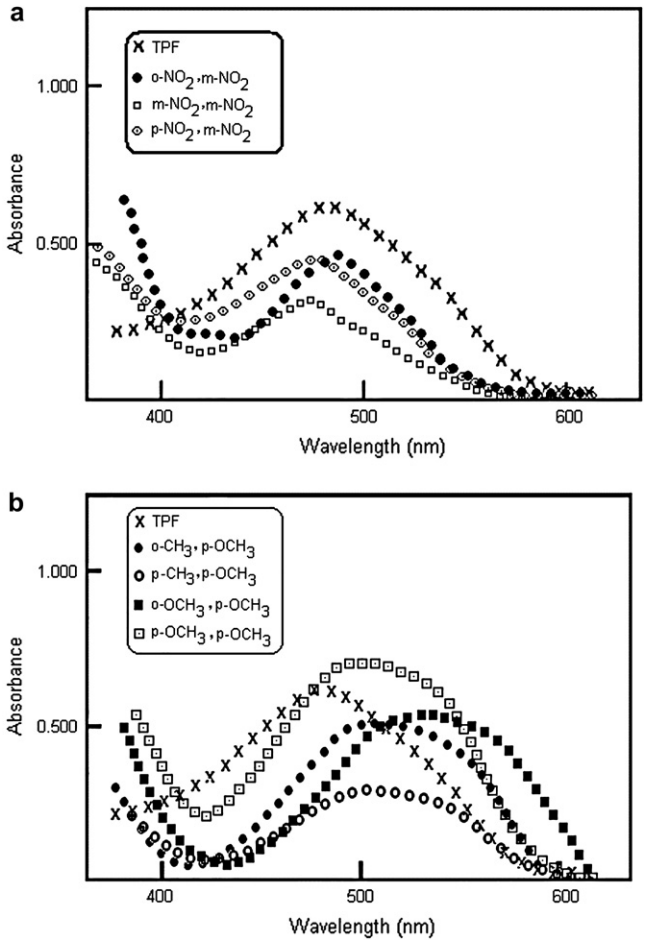


Fig. 2. UV–vis spectra of: (a) compounds **1–4** compared to TPF; (b) compounds **11**, **13**, **14** and **16** compared to TPF.

486 nm and acted as electron donating groups due to resonance effect (compounds **7** and **10**).

In compounds **11–13** where 1-phenyl ring is substituted with $-CH_3$ group at *o*-, *m*- and *p*-position and 3-phenyl ring is substituted with $-OCH_3$ group at *p*-position the $\lambda_{max}$ values were shifted to 512, 504 and 501 nm, respectively, in accordance with the electron donating effects of both groups. The $\Delta\lambda_{max}$ shift values were observed to be 30, 22 and 19 nm for *o*-, *m*- and *p*-position. The gradual decrease in the shift values from *o*- to *p*-position can be attributed to the gradual decrease in the inductive electron donating properties of $-CH_3$ and $-OCH_3$ as they move from the center.

In compounds **14–16** where the 1-phenyl ring is substituted with an $-OCH_3$ group at *o*-, *m*-, and *p*-position and 3-phenyl ring is substituted with an $-OCH_3$ group at *p*-position the $\lambda_{max}$ values were shifted to 531, 507 and 499 nm, respectively, in accordance with the electron donating effects of both groups. This results in $\Delta\lambda_{max}$ shift values of 49, 25 and 17 nm according to *o*-, *m*-, and *p*-position. The reduction of the shift values from *o*- to *p*-position is in good accordance with the fact that the inductive electron donating effect of the $-OCH_3$ group decreases as it moves away from the center. Fig. 2b compares the $\lambda_{max}$ values of *o*- and *p*-position of $-CH_3$ and $-OCH_3$ groups. All of UV–vis $\lambda_{max1}$ values are against TPF at the Fig. 3 for compared.

## 3. Conclusions

### *3.1. The relation between the $\Delta\lambda_{max}$ values and Hammett substituent coefficients—$\sigma$*

Hammett substituent coefficients ($\sigma$) are used to evaluate the effect of the substituents upon the rate of a chemical reaction for which mechanism is known. If positive is $\sigma$ value of the substituent is electron withdrawing, then it exerts a hypsochromic effect upon the $\lambda_{max}$ values. The amount of shift in $\lambda_{max}$ values and the magnitude of $\Delta\lambda_{max}$ values are proportional to the electron withdrawing ability of the substituent depending upon its type and position. When only inductive effect was present the value of $\Delta\lambda_{max}$ is small. The presence of resonance effect increases the value of chemical shift. The highest $\Delta\lambda_{max}$ value is observed when both inductive and resonance effects come together. In our previous study we emphasized that electron donating groups caused bathochromic effect upon $\Delta\lambda_{max}$ values [17,18]. Therefore, the substitution of electron donating groups upon formazan molecule increases conjugation and the photosensitization and causes a bathochromic effect upon $\lambda_{max}$. On the other hand the electron withdrawing groups decrease the conjugation and thus photosensitization and cause a hypsochromic effect upon $\lambda_{max}$ values [19,23].

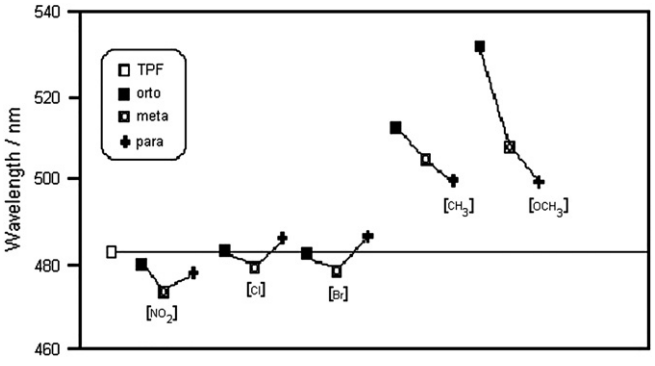


Fig. 3. Comparison of $\lambda_{max}$ values of substituted formazans with TPF.

We wanted to investigate whether we could use the Hammett substituent coefficients in order to evaluate the total effect of two different substituents, upon the $\lambda_{max}$ values and thus the color. Hammett substituent coefficient $\sigma$ has been related with $\lambda_{max}$ values for only one substituent in the structure up to now. This study as far as our knowledge is the first one to investigate the relation between total $\sigma_T$ ($\sigma_1 + \sigma_2 = \sigma_T$) and $\lambda_{max}$ when two different phenyl rings are attached with two different substituents at different positions. The total $\sigma_T$ and related $\lambda_{max}$ values are given in Table 5. The total $\sigma_T$ and related $\lambda_{max}$ values are plotted in Fig. 4.

As seen from Fig. 4 there is a linear relation between $\sigma_T$ and $\lambda_{max}$ values. Therefore, $\sigma_T$ values can be used to evaluate the absorption $\lambda_{max}$ values.

As seen from Fig. 4 there is a linear correlation between Hammett substituent coefficient $\sigma_T$ and $\lambda_{max}$ except in *m*-$OCH_3$. This shows that it is possible to use the summation of Hammett substituent coefficient $\sigma_T$ ($\sigma_1 + \sigma_2 = \sigma_T$).

## 4. Experimental

### *4.1. General*

The UV–vis spectra of the formazans synthesized in this study were obtained with UNICAM UV2-100 UV–vis spectrophotometer using 1 cm quartz cells in $10^{-5}$ mol $l^{-1}$ $C_3H_6O$ using 325 nm lamp in the range of 250–600 nm. The IR spectra were obtained on a MATT-SON 100-FT-IR spectrophotometer between 4000 and 400 $cm^{-1}$ using KBr pellets. $^1H$ NMR spectra were performed on a Bruker AVANCE DPX-400 MHz and $^{13}C$ NMR 100 MHz spectrophotometer using $CDCl_3$ and DMSO-$d_6$, $10^{-4}$ mol $l^{-1}$. The elemental analysis was carried out by LECO-CHNS-932 elemental analyser. Mass spectra were recorded using an AGILENT 1100 MSD mass spectrometer.

### *4.2. General synthesis*

Synthesis was carried out using benzaldehyde (or substituted benzaldehydes), phenylhydrazine and aniline (or substituted anilines). Benzaldehyde (or substituted benzaldehydes) was reacted with phenylhydrazine at pH 5–6 to obtain benzaldehyde phenylhydrazone (or substituted benzaldehyde phenylhydrazones). These hydrazones were then coupled with benzene diazonium chloride at 0–5 °C.

Table 5
The total $\sigma_T$ ($\sigma_1 + \sigma_2 = \sigma_T$) and related $\lambda_{max}$ values

| Substituent position | Compound | Abbreviation | $\sigma'$ value | $\sigma_T$ (Total effect) | $\lambda_{max1}$ (nm) |
|---|---|---|---|---|---|
| *m* | **1** | H | H: 0 | 0 | 482 |
| | **3** | *m*-$NO_2$, *m*-$NO_2$ | *m*-$NO_2$: 0.71; *m*-$NO_2$: 0.71 | 1.42 | 473 |
| | **6** | *m*-Cl, *m*-$NO_2$ | *m*-Cl: 0.37; *m*-$NO_2$: 0.71 | 1.08 | 480 |
| | **9** | *m*-Br, *m*-$NO_2$ | *m*-Br: 0.37; *m*-$NO_2$: 0.71 | 1.08 | 479 |
| | **12** | *m*-$CH_3$, *p*-$OCH_3$ | *m*-$CH_3$: −0.06; *p*-$OCH_3$: −0.12 | −0.18 | 504 |
| | **15** | *m*-$OCH_3$, *p*-$OCH_3$ | *m*-$OCH_3$: 0.10; *p*-$OCH_3$: −0.12 | −0.02 | 507 |
| *P* | **4** | *p*-$NO_2$, *m*-$NO_2$ | *p*-$NO_2$: 0.81; *p*-$NO_2$: 0.71 | 1.52 | 478 |
| | **7** | *p*-Cl, *m*-$NO_2$ | *p*-Cl: 0.24; *p*-$NO_2$: 0.71 | 0.95 | 486 |
| | **10** | *p*-Br, *m*-$NO_2$ | *p*-Br: 0.26; *p*-$NO_2$: 0.7 | 0.97 | 486 |
| | **13** | *p*-$CH_3$, *p*-$OCH_3$ | *p*-$CH_3$: −0.14; *p*-$OCH_3$: −0.12 | −0.26 | 501 |
| | **16** | *p*-$OCH_3$, *p*-$OCH_3$ | *p*-$OCH_3$: −0.12; *p*-$OCH_3$: −0.12 | −0.24 | 499 |

*4.2.1. Synthesis of 1,3,5-triphenylformazan (**1**)*

1,3,5-Triphenylformazan was synthesized by the reaction of benzaldehyde (1.06 g, 0.01 mol), phenylhydrazine (1.08 g, 0.01 mol), aniline (0.93 g, 0.01 mol) concentrated HCl (5 ml) and sodium nitrite (0.75 g) in a methanol at 0–5 °C, like in lit. [19].

*4.2.2. Synthesis of 1-(o-, m-, p-nitrophenyl)-3-(m-nitrophenyl)-5-phenylformazans (**2–4**)*

*m*-Nitrobenzaldehyde (1.51 g, 0.01 mol) was dissolved in methanol (25 ml) and phenylhydrazine (1.08 g, 0.01 mol) was gradually added with constant stirring at pH 5–6. The procedure was completed in 30 min. The resulting blood-red hydrazone was left on the bench overnight and then was filtered and recrystallised from methanol. The *m*-nitrobenzaldehydephenylhydrazone (2.41 g, 0.01 mol) was dissolved in methanol (50 ml) by constant stirring under reflux and buffer solution (prepared as before). In another flask *o*-, *m*-, *p*-nitrobenzenediazonium chloride solutions were prepared using *o*-, *m*-, *p*-nitroaniline (1.38 g, 0.01 mol) concentrated HCl (5 ml) and sodium nitrite (0.75 g) at 0–5 °C. This solution was added to the *m*-nitrobenzaldehyde phenylhydrazone solution drop wise with constant stirring to form compounds. The solution was stirred for 2 h at the same temperature and kept in a cupboard for 2 days. Each compound was recrystallised from methanol. Elemental analysis for $C_{19}H_{14}N_6O_4$, Calc. (%): C, 58.46; H, 3.59; N, 21.54. Found: (%) C, 58.50; H, 3.56; N, 21.50. Calc. M: 390.0. Found: mass: *m/z* (eV): 391.1, 241.0, 150.0, 108.0.

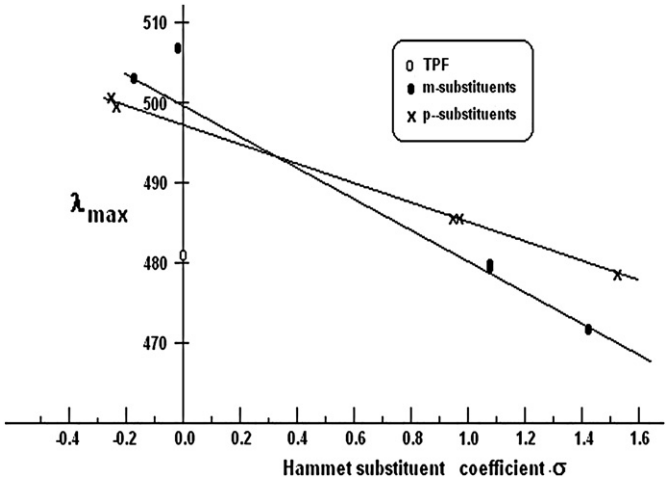


Fig. 4. The comparison of $\lambda_{max}$ values against $\sigma$.

*4.2.3. Synthesis of 1-(o-, m-, p-chlorophenyl)-3-(m-nitrophenyl)-5-phenylformazans (**5–7**)*

*m*-Nitrobenzaldehyde (1.51 g, 0.01 mol) was dissolved in methanol (25 ml) and reacted with phenylhydrazine (1.08 g, 0.01 mol) to give *m*-nitrobenzaldehyde phenylhydrazone. The *m*-nitrobenzaldehyde phenylhydrazone (2.41 g, 0.01 mol) was dissolved in methanol (50 ml). In another flask *o*-, *m*-, *p*-chlorobenzenediazonium chloride solutions were prepared using *o*-, *m*-, *p*-nitroaniline (1.27 g, 0.01 mol). This solution was added to the *m*-nitrobenzaldehyde phenylhydrazone solution. The procedure was like as mentioned earlier in Section 4.2.2. Elemental analysis for $C_{19}H_{14}N_5O_2Cl$, Calc. (%): C, 60.08; H, 3.69; N, 18.44. Found: (%) C, 60.13; H, 3.73; N, 18.50. Calc. M: 379.5. Found: mass: *m/z* (eV): 380.1, 274.0, 139.0, 126.0.

*4.2.4. Synthesis of 1-(o-, m-, p-bromophenyl)-3-(m-nitrophenyl)-5-phenylformazans (**8–10**)*

*m*-Nitrobenzaldehyde (1.51 g, 0.01 mol) was dissolved in methanol (25 ml) and reacted with phenylhydrazine (1.08 g, 0.01 mol) to give *m*-nitrobenzaldehyde phenylhydrazone. The *m*-nitrobenzaldehyde phenylhydrazone (2.41 g, 0.01 mol) was dissolved in methanol (50 ml) In another flask *o*-, *m*-, *p*-bromobenzenediazonium chloride solutions were prepared using *o*-, *m*-, *p*-bromoaniline (1.75 g, 0.01 mol). This solution was added to the *m*-nitrobenzaldehyde phenylhydrazone solution. The procedure was like as mentioned earlier in Section 4.2.2. But each compound was recrystallised from dioxan. Elemental analysis for $C_{19}H_{14}N_5O_2Br$, Calc. (%): C, 53.77; H, 3.30; N, 16.51. Found: (%) C, 53.70; H, 3.27; N, 16.55. Calc. M: 424. Found: mass: *m/z* (eV): 425.0, 318.3, 240.0, 170.1.

*4.2.5. Synthesis of 1-(o-, m-, p-tolyl)-3-(p-methoxyphenyl)-5-phenylformazans (**11–13**)*

*p*-Methoxybenzaldehyde (1.35 g, 0.01 mol) was dissolved in methanol (30 ml) and reacted with phenylhydrazine (1.08 g, 0.01 mol) to give *p*-methoxybenzaldehydephenylhydrazone.

It was then coupled with equivalent amounts of *o*-, *m*-, *p*-tolyldiazonium chloride at 0–5 °C giving purple coloured formazans. The procedure was like as mentioned earlier in Section 4.2.2. Elemental analysis for $C_{21}H_{20}N_4O$, Calc. (%): C, 70.00; H, 5.55; N, 15.55. Found: (%) C, 70.06; H, 5.51; N, 15.62. Calc. M: 360. Found: mass: *m*/*z* (eV) 361.1, 255.1, 225.1, 122.1.

*4.2.6. Synthesis of 1-(o-, m-, p-methoxyphenyl)-3-(p-methoxyphenyl)-5-phenylformazans (**14–16**)*

*p*-Methoxybenzaldehyde (1.35 g, 0.01 mol) was dissolved in methanol (30 ml) and reacted with phenylhydrazine (1.08 g, 0.01 mol) to give *p*-methoxybenzaldehyde phenylhydrazone. It was then coupled with equivalent amounts of *o*-, *m*-, *p*-methoxybenzenediazonium chloride at 0–5 °C giving purple coloured formazans. The procedure was like as mentioned earlier in Section 4.2.2. Elemental analysis for $C_{21}H_{20}N_4O_2$, Calc. (%): C, 73.25; H, 5.81; N, 16.28. Found: (%) C, 73.21; H, 5.76; N, 16.24. Calc M: 344. Found mass: *m*/*z* (eV): 345.1, 239.1, 225.0, 119.

## Acknowledgements

We are very grateful to Gazi University Research Fund for providing financial support for this Project (No. 04/2004-13) and Prof. Dr. M. Levent Aksu for precious assisting.

## References

[1] Von Pechmann H. Ber Dtsch Chem Ges 1894;27:1679.
[2] Hunter L, Roberts CB. J Chem Soc 1941;9:820–3.
[3] Lewis JW, Sandorfy C. Can J Chem 1983;61:809–16.
[4] McConnachie G, Neuqebauer FA. Tetrahedron 1975;31:555–60.
[5] Katritzky AR, Belyakov SA, Cheng D, Durst HD. Synthesis 1995;5:577–81.
[6] Ibrahim YA, Abbas AA, Elwahy AHM. J Heterocycl Chem 2004;41:135–49.
[7] Elwahy AHM, Abbas AA. Tetrahedron Lett 2006;47:1303–6.
[8] Barsoum BN, Khella SK, Elwaby AHM, Abbas AA, Ibrahim YA. Talanta 1998;47:1215–22.
[9] Czajkowski W, Stolarski R, Szymczyk M, Wrzeszcz G. Dyes Pigments 2000;47:143–9.
[10] Szymczyk M, El-Shafei A, Freeman HS. Dyes Pigments 2006;7:206–13.
[11] Schiele VC. Ber 1964;30:308–18.
[12] Mattson AM, Jensen CO, Dutcher RA. Science 1947;5:294–5.
[13] Plumb JA, Milray R, Kaye SB. Cancer Res 1989;49:4435–40.
[14] Wan H, Williams R, Doherty P, Williams DF. J Mater Sci Mater Med 1994;5:154–9.
[15] Aziz DM. Anim Reprod Sci 2006;92:1–8.
[16] Yüksel U. Post doctoral thesis. Aegean University; 1981 [Turkish].
[17] Tezcan H, Uyar T. Turkish J Spect Aegean University 1988;9:8–19; Tezcan H, Uyar T, Tezcan R. Turkish J Spect Aegean University 1989;10:82–90.
[18] Tezcan H, Can S, Tezcan R. Dyes Pigments 2002;52:121–7.
[19] Tezcan H, Ozkan N. Dyes Pigments 2003;56:159–66.
[20] Tezca H, Ozbek N. Commun Fac Sci Univ Ank Ser B 2005;51:13–28.
[21] Gokce G, Durmus Z, Tezcan H, Kilic E, Yılmaz H. Anal Sci 2005;21:1–4.
[22] Erkoc S, Tezcan H, Calisir ED, Erkoc F. Int J Pure Appl Chem 2006;1(1):37–44.
[23] Williams DH, Fleming I. Spectroscopic methods in organic chemistry. London: McGraw-Hill Publishing Company Limited; 1966.
[24] Schiman F. Nuclear magnetic resonance of complex molecules, vol. 1. Braunschweig: Vieweg and Sohn GmbH; 1970.
[25] Bellamy LJ. The infrared spectra of complex molecules. London: Methuen; 1962.